pH sensitivity of YFPs is reduced upon AlphaRep binding: proof of concept in vitro and in living cells

Yasmina Bousmah, Magali Noiray, Hadrien Jalaber, Hélène Pasquier, Marie Béatrice Valerio-Lepiniec, Agathe Urvoas, Marie Erard

pH sensitivity of YFPs is reduced upon AlphaRep binding: proof of concept in vitro and in living cells

Yasmina Bousmah[a], Magali Noiray[b], Hadrien Jalaber[a], Hélène Pasquier[a], Marie Béatrice Valerio-Lepiniec[b], Agathe Urvoas[b], Marie Erard[a]

Affiliations

[a]Université Paris-Saclay, Institut de Chimie Physique, UMR 8000 CNRS, 91405, Orsay, France

[b]Université Paris-Saclay, CEA, CNRS, Institute for Integrative Biology of the Cell (I2BC), 91198 Gif-sur-Yvette, France

E-mail: marie.erard@universite-paris-saclay.fr

Abstract (max 200 words)

Yellow fluorescent proteins (YFPs) are commonly used in biology to track cellular processes, particularly as acceptors in experiments using the Förster Resonant Energy Transfer (FRET) phenomenon. However, their fluorescence intensity is strongly pH-dependent, limiting their utility in acidic environments. Here, we explore the pH sensitivity of YFPs upon binding with an artificial repeat protein (αRep) both *in vitro* and in living cells. We show that αRep binds to Citrine, with high affinity in the nanomolar range at physiological and acidic pHs, leading to increased thermal stability of the complex. Moreover, αRep binding reduces Citrine's pK_a by 0.75 pH units, leading to a decreased sensitivity to pH fluctuations. This effect can be generalized to other YFPs as Venus and EYFP *in vitro*.

An efficient binding of αRep to Citrine has also been observed in living cells both at pH 7.4 and pH 6. This interaction leads to reduced variations of Citrine fluorescence intensity in response to pH variations in cells.

Overall, the study highlights the potential of αReps as a tool to modulate the pH sensitivity of YFPs, paving the way for future exploration of biological events in acidic environments by FRET in combination with a pH-insensitive cyan donor.

Keywords

Fluorescent protein, YFP, alphaRep (αRep), pH sensitivity, FRET, FLIM

Introduction

Fluorescent proteins (FPs) serve as genetically encoded fluorescent reporters and have been invaluable tools in cell biology for more than 25 years, enabling researchers to visualize and track various cellular processes with remarkable spatial and temporal resolution.[1] Their chromophore is formed by the autocatalytic reaction of three residues embedded in their *β*-barrel structure at positions 65-66-67. Typically, position 66 is occupied by a tyrosine, and upon chromophore formation, its electron delocalization expands on two additional double bonds leading to a moiety capable of absorbing and fluorescing in the visible. Depending on the pH and its environment in the *β*-barrel, the chromophore may adopt an anionic or a protonated form, both having different photophysical properties (Figure 1a). Fluorescent proteins with an excitation maximum of 515 ±5 nm are usually considered yellow fluorescent proteins (YFP). Those YPFs are an advantageous label combined with more blue or red FPs for multicolor labeling and the usual acceptor in combination with a cyan donor in Förster Resonant Energy Transfer (FRET) experiments.[2] Despite their good brightness (Epsilon above 75 000 $mol.L^{-1}.cm^{-1}$ et QY generally exceeding 0.65)[3], their absorption and fluorescence strongly depend on pH due to the equilibrium between the anionic and fluorescent form of the chromophore and its protonated but nonfluorescent form.[1] The pK_a is the pH at which 50% of the protein fluoresces when they are excited in their anionic absorption band. All YFPs derived from *av*GFP have a $pK_a > 5$ [3], even Citrine, one of the best, as far as the pH sensitivity is concerned [4]. This strongly limits their use in the acidic compartments present in many cell types, such as the granules in the secretion pathway in eukaryotic cells [5] or the vacuole in plant cells[6] or in a cytoplasmic context where local proton concentration may be high or fluctuating due to intense enzymatic activity for example. In addition, the pH sensitivity of YFPs impacts their use as a FRET acceptor in acidic conditions: the modification of their absorption band at a low pH decreases the spectral overlap with the donor fluorescent band leading to the apparent decrease of the FRET efficiency independently from the monitoring of any biological event.[7] Intense engineering has been undertaken to limit and control the sensitivity of YFPs -and, more generally, FPs- to pH fluctuations.[8] Recently, tdLanYFP, a YFP with a very low $pK_a = 3.9$ was characterized.[9] Other strategies rely on the interaction with a small partner protein, such as a nanobody.[10–12] They modulate the FP properties such as brightness, switching rate between two fluorescent states, and also their pK_a.[10–12]

In this manuscript, we focus on artificial repeat proteins (αRep).[13] Their alpha-helicoidal HEAT-like repeat sequence is coding for a motif of 31 residues containing five highly variable positions. A library of αReps with diversity in the number of inserted repeats and the sequence at the variable positions was built as a large source of protein binders (>1 billion clones).[14] Here, we focus on bGFP-C, an αRep selected to bind specifically *in vitro* and *in cellulo* to EGFP, a FP belonging to the avGFP family.[15] The X-ray structure of this αRep in interaction with EGFP has been solved (Figure 1b). bGFP-C binds EGFP on the edge of the *β*-barrel, mainly on strands 7, 8, and 9. The 7^{th} strand (in red Figure 1b) is in front of the phenol moiety of the chromophore and mutations in this strand may impact the biochemical and photophysical behavior of the chromophore.[12] In particular, this strand is usually chosen to insert a sensing protein in cpFPs to build biosensors,[16] showing the importance of its residues in modulating the properties of the chromophore itself. In addition, the dissociation constant of the bGFP-C / EGFP complex is in the nM range and bGFP-C displays interactions with similar

affinities for other members of the *av*GFP family such as EYFP and ECFP, which share a very close sequence and protein surface.[3] bGFP-C is called simply αRep hereafter.
We hypothesized that the binding of αRep to YFPs could lead to altered properties that may improve their pK_a for fluorescence imaging in acidic compartments. In this work, we, therefore, set out experiments to examine the effect of αRep on YFPs. We chose the popular Citrine as a model, and our observations will be generalized *in vitro* to other YFPs from the same family, namely EYFP and Venus (Figure S1). A proof of concept in living cells is presented with Citrine.

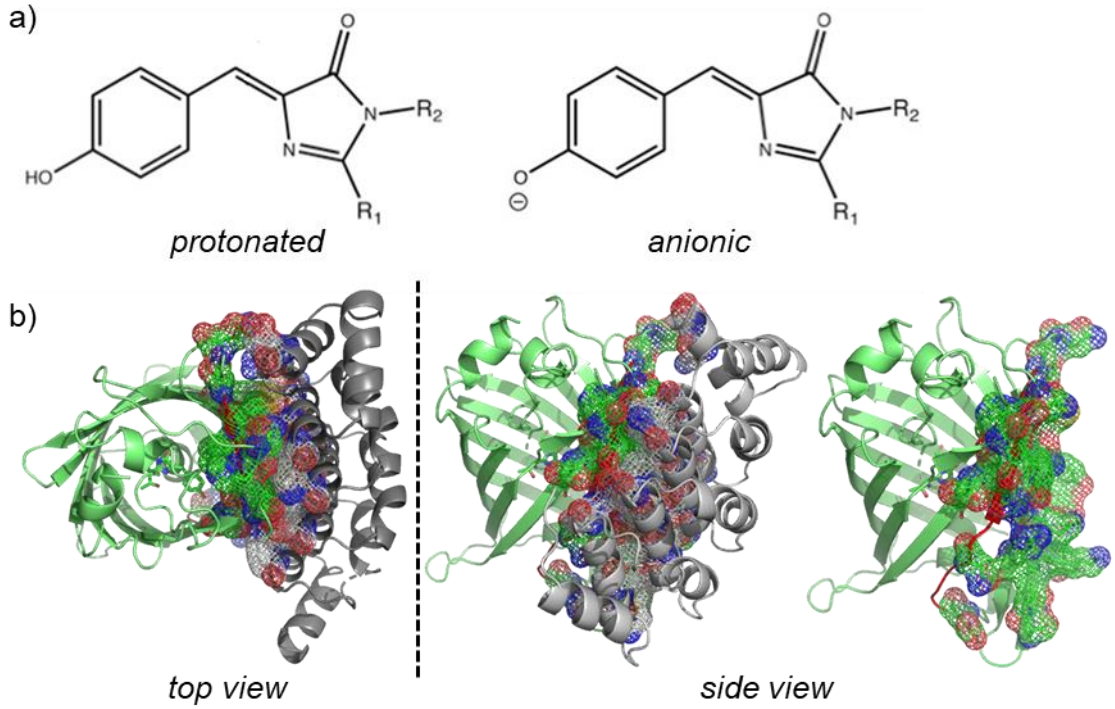

Figure 1: (a) Protonated nonfluorescent and anionic fluorescent chromophores of YFPs. (b) Structure of EGFP (green) - αRep complex, top and side views (pdb 4XVP). The residues in interaction are represented in a mesh. The 7th strand of the β-barrel, in front of the chromophore, is in red on the side view mostly hidden by residues in interaction.

Experimental section

Plasmids

EYFP, Citrine, and Venus refer to three yellow fluorescent proteins (YFPs).[3] For bacterial expression, YFPs were cloned in pProExHTa. αRep variants bGFPC-GFP (called **αRep)**[15] and bNCS324-16 (called **control αRep)**[14] genes were subcloned in pQE81L vectors (Qiagen). All proteins are produced as His-tagged proteins. For eukaryotic expression, pECitrine-N1 (Clontech) was used. αRep was subcloned in a modified pmCherry-N1 vector (Clontech).[15] All the protein sequences are in Figure S1.

Protein expression and purification

The production and the purification of His-tagged recombinant YFPs were performed as previously described.[17] The elution buffer is replaced by a buffer composed of a mixture of 2 mM CAPS, 2 mM MES, and 2 mM Bis–tris propane, pH 7.4. As the values of the epsilons for FPs vary from one publication to the other in a 10-20% range,[3,9,18] we used an average epsilon of 80 000 $mol^{-1}.L.cm^{-1}$ at the maximum of the chromophore's absorption spectrum to determine the concentration of all YFPs before each experiment when needed.

The production and the purification of His-tagged recombinant αRep were adapted from a previous work.[15] In the first step, the plasmid coding for each protein was transformed into the expression strain (*E.coli* M15). An overnight pre-culture of a clone was grown at 37°C in 50 mL of 2YT medium containing 100 μg/mL ampicillin and 1% of glucose. For expression, 25 mL of bacteria were grown at 37°C in 1 L of 2YT medium containing 100 μg/mL ampicillin, at 200 rpm, up to an OD of 0.6 at 600 nm. The addition of 0.5 mM IPTG induced protein expression. The cells were further incubated for four hours at 37°C. Then the culture was centrifuged for 30 minutes at 5000 g, 4°C. The bacterial pellet was harvested, resuspended in 20 mL of a buffer containing antiprotease tablet (cOmplete Protease Inhibitor Cocktail, Roche), Tris 20 mM, and NaCl 200 mM at pH 7.5 and frozen at -80°C for several days. The bacterial pellet was resuspended in buffer (40 mL, Tris 20 mM, NaCl 200 mM, pH 7.5, DNase 0.5 mg/mL) and lysed with a cell disruptor (Constant Systems Ltd). The cell debris was removed by centrifugation for 30 minutes at 10 000 g, 4°C. The supernatant was filtered and then applied to a chromatography column containing nickel-nitriloacetic acid (Ni–NTA) agarose beads (His Trap FF crude, GE Healthcare) for 1 hour. The protein was eluted with a phosphate buffer at pH 8 containing 300 mM NaCl and 300 mM imidazole. This purification was further carried out with size exclusion chromatography (Hiload 16/600 SuperdexTM 75 Cytivia) using a buffer composed of Tris 10 mM, NaCl 150 mM at pH 7.5. SDS-PAGE of the purified protein shows a single band between15 kDa and 18 kDa for bGFPC and bNCS324-16.

Differential Scanning Calorimetry and Isothermal Titration Calorimetry

For differential scanning calorimetry (DSC) and isothermal titration calorimetry (ITC), proteins have been prepared in buffers containing the same mixture of CAPS 33 mM, MES 33 mM, Bis–tris propane 33 mM, and NaCl 50 mM adjusted at pH 7.4 or pH 5.5. To avoid any aggregation of Citrine at pH 5.5, a pH close to the pI, four short-time dialysis (two hours) of the stock solution (concentration ~350 µM) at pH 5.5 were preferred instead of a single one

overnight. The αRep followed the same process. At pH 7.4, two long-time dialyses were performed. The final pH of the protein solutions and their concentration were accurately monitored just before each experiment.

Thermal stability of Citrine at 20 µM, αRep at 20 µM and complex Citrine - αRep at 1:1 molar ratio (20µM:20µM) was performed by DSC on an auto PEAQ DSC (Malvern Panalytical, France). Each measurement was completed by a baseline scan with the sample buffer.

Scans were performed at 1°C min^{-1} between 35 and 120◦C. The heat capacity of the buffer was subtracted from that of the protein sample before analysis. Analysis of the raw data was performed using the Microcal PEAQ-DSC software v1.63. T_m is the temperature at which half of the protein is denaturated.

The binding parameters were assessed at 25°C with a MicroCal PEAQ-ITC instrument (Malvern Panalytical, France). Aliquots (2 µL) of Citrine at high concentration were placed in the 40µL injection syringe and were injected every 180 s into a 20 µM αRep solution (cell volume, 0.24 mL), under a stirring speed of 500rpm, using the Microcal PEAQ-ITC Control software v.1.41. Citrine's concentrations were 320 µM at pH 7.4 and 230 µM at pH 5.7. Analysis of the raw data was performed using the Microcal PEAQ-ITC analysis software v.1.41 according to the one set of sites binding model.

Absorption and fluorescence spectroscopies and pK_a determination

The spectra were recorded with a SynergyH1 plate reader (Biotek) in 96-transparent-well plates and spectra were processed as previously described.[7] Absorption spectra were recorded from 350 nm to 560 nm and fluorescence emission spectra from 515 nm to 670 nm upon excitation at 480 nm. Fluorescence lifetimes were recorded on a TCSPC setup described elsewhere,[19] with an excitation at 515±10 nm and an emission at 535±3 nm. The decays were fitted with SymPhoTime software with a single exponential. For pH levels ranging from pH 11 to pH 5.5, buffer solutions contained 33 mM CAPS, 33 mM MES, and 33 mM Bis–tris propane and were adjusted to the appropriate pH by the addition of H_2SO_4 or NaOH. For pH levels ranging from 5.5 to 2.5, buffer solutions consisted of 50 mM citric acid with an appropriate volume of Na_2HPO_4 to adjust the pH. In those buffers, the residual chloride concentrations were below 20 mM depending on the final concentration of αRep. The molar ratio YFP:αRep in the solution is 1:1. Aliquots from a concentrated stock protein solution were diluted into the different buffers at least 12 h before measurements. After a first series of measurements at low chloride concentration, a solution at 6 M NaCl was added to adjust the $[Cl^-]$ concentration to 200 mM. For the determination of pK_a, the variation of the absorbance with the pH was fitted with IgorPro*V6* Software (Wavemetrics) according to the following equation (1):

$$A(pH) = \frac{A_{max}^{Basic} + A_{min}^{Acid} 10^{n_{Hill} \times (pKa - pH)}}{1 + 10^{n_{Hill} \times (pKa - pH)}} \quad (1)$$

Live cell imaging and cytometry

Live cell experiments were performed in COS7 cells transiently transfected with XTremeGene HT (ThermoFisher) following the manufacturer's protocol. The cytosolic pH of COS7 cells was modified by a method based on the K^+/H^+ ionophore nigericin (final concentration 15 µM) in

the presence of a buffer (HEPES 15 mM and MES 15 mM) at pH 8 to pH 5.5 containing external potassium ions (140 mM KCl). FLIM experiments were performed on a homemade TCSPC setup described previously.[20] Citrine was excited at 466 nm with a pulsed diode (Picoquant) and its fluorescence was detected with a 535/40 nm bandpass filter. SymPhoTime64 software (Picoquant) was used for data acquisition and processing. The fluorescence intensity of αRep-mCherry was monitored with a CCD camera (Orca, Hamamastu) with a Chroma filter set for RFPs (ET580/25x for excitation, ET625/30m for emission and ZT594rdc for the dichroic mirror). FastFLIM lifetime images and histograms were calculated for all pixels above 500 cps by SymPhoTime64 software. For each cell, a single TCSPC fluorescence decay gathers all the photons collected from cytosolic Citrine. For cells expressing Citrine alone, the decays are fitted with a mono-exponential fit function (2) to compute the lifetime of Citrine alone, $\tau_{Citrine}$:

$$I(t) = Background + I_0 e^{-\frac{t}{\tau_{Citrine}}} \qquad (2)$$

For cells expressing both Citrine and αRep-mCherry, bi-exponential fit function (3) was used:

$$I(t) = Background + I_0 \times (\alpha_1\, e^{-\frac{t}{\tau_1}} + \alpha_2\, e^{-\frac{t}{\tau_2}}) \qquad (3)$$

The average lifetime is computed as $< \tau_{Citrine\ with\ \alpha\text{Rep} - \text{mCherry}} >= \alpha_1\, \tau_1 + \alpha_2\, \tau_2$. The quality of the fit is evaluated by the weighted residual distribution and Pearson's χ^2 test. The apparent FRET efficiency is then calculated with equation (4) for each cell:

$$E_{FRET}^{Apparent} = 1 - \frac{<\tau_{Citrine\ with\ \alpha\text{Rep} - \text{mCherry}}>}{\tau_{Citrine}} \quad (4)$$

For wide-field fluorescence microscopy and flow cytometry experiments, cells were transfected either with plasmids coding for Citrine or for both Citrine and αRep-mCherry with a 1:3 DNA ratio. For wide-field microscopy, cells were observed successively with Citrine and mCherry filters (filters YFP2427B Semrock for Citrine and filters ET580/25X and ET625/30 Semrock for mCherrry) at pH 7.4 and 15 min after the addition of an excess of buffer at pH 5.5 in the presence of 15 µM nigericin, leading to a final pH below pH6. For flow cytometry, cells were trypsinized 24 h after transfection. 5 min before the analysis, the intracellular pH was modified with a buffer at the appropriate pH in the presence of nigericin. Flow-cytometry measurements were done on a Cytoflex S instrument with the CytExpert software (Beckman Coulter), using a 488 nm laser excitation and a 525/40 BP emission filter for Citrine and a 561 nm laser excitation and a 610/20 BP emission filter for mCherry. The data processing was performed using FloJow software (BDbiosciences). Living cells were identified with the Forward Scatter (FCS) and Side Scatter (SSC) channels and fluorescent cells in both, Citrine and mCherry, channels were chosen to calculate the averaged Citrine fluorescence intensity.

Results

αRep binds Citrine at physiological and acidic pHs

DSC experiments were first performed to probe the Citrine - αRep interaction at physiological and acidic pHs (Figure 2, Table 1). The melting temperature (T_m) of the heating thermogram of Citrine alone slightly decreases from 78°C at pH 7.4 to 64°C at pH 5.5 showing that Citrine is a less structured protein at low pH. On the other hand, the T_m of αRep increases from 83°C to 88°C from pH 7.4 to pH 5.5 indicating a slightly higher stability at the lower pH value. At pH 7.4, the equimolar mixture of Citrine and αRep presents a single transition centered at 83°C associated with an increased ΔH of 386 kcal.mol^{-1}. The shift of the mixture thermogram compared to one of Citrine alone is consistent with the formation of a stabilized complex between both proteins. At pH 5.5, two principal peaks, at T_{m1} = 74°C and T_{m2} = 88°C, are observed for the mixture that starts to melt around 50°C, a temperature lower than that at pH 7.4. The interaction between Citrine and αRep is thus less efficient at lower pHs. Nevertheless, T_{m1} is still higher than the one for Citrine alone: the interaction of αRep with Citrine leads to a stabilized structure, also at low pHs, down to pH 5.5. T_{m2} is likely the melting temperature of free αRep. The shoulder at 65°C could be attributed to a small fraction of free Citrine at the lower pH.

	Physiological pH			Acidic pH		
	T_m / °C	ΔH / kcal.mol^{-1}	K_D / nM	T_m / °C	ΔH / kcal.mol^{-1}	K_D / nM
Citrine	78	159		64	160	
αRep	83	157		88	165	
Citrine - αRep	83	386	48 ± 7	(1) 74 (2) 88	(1) 253 (2) 173	137 ± 9

Table 1: Melting temperatures (T_m) and variations of melting enthalpy (ΔH) measured by DLS, and K_D measured by ITC of Citrine, αRep, and Citrine – αRep complex at physiological and acidic pHs. For acidic pHs, T_m and ΔH were estimated at pH 5.5 and K_D at pH 5.7.

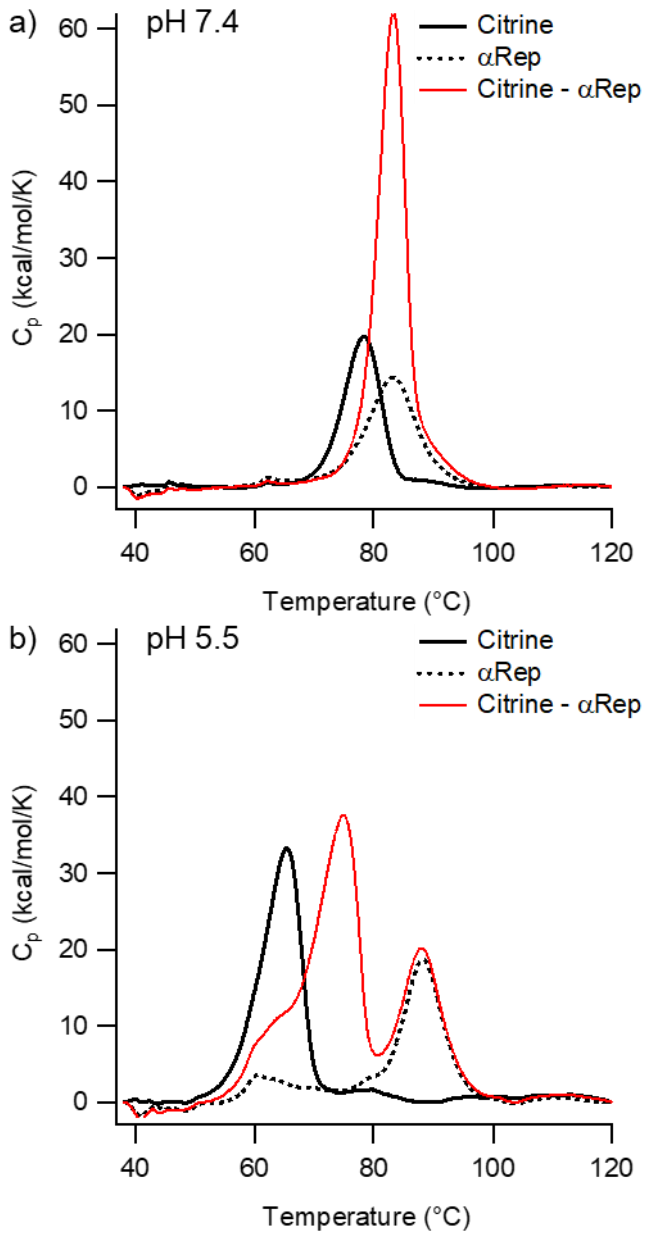

Figure 2: Heating thermograms of Citrine, αRep, and an equimolar mixture of Citrine and αRep at pH 7.4 (a) and pH 5.5 (b), proteins concentration: 20 µM.

To confirm those first observations, ITC experiments were performed to determine the affinity parameters of Citrine for αRep in physiological (pH 7.4) and acidic conditions (pH 5.7) (Figure 3). The dissociation constants are in the nanomolar range, with K_D values of 48 ± 7 nM and 137 ± 9 nM and stoichiometry values (n) of 1.3 and 0.8 at pH 7.4 and pH 5.7 respectively. A clear exothermic interaction with the formation of nearly equimolar complexes was observed at both pHs.

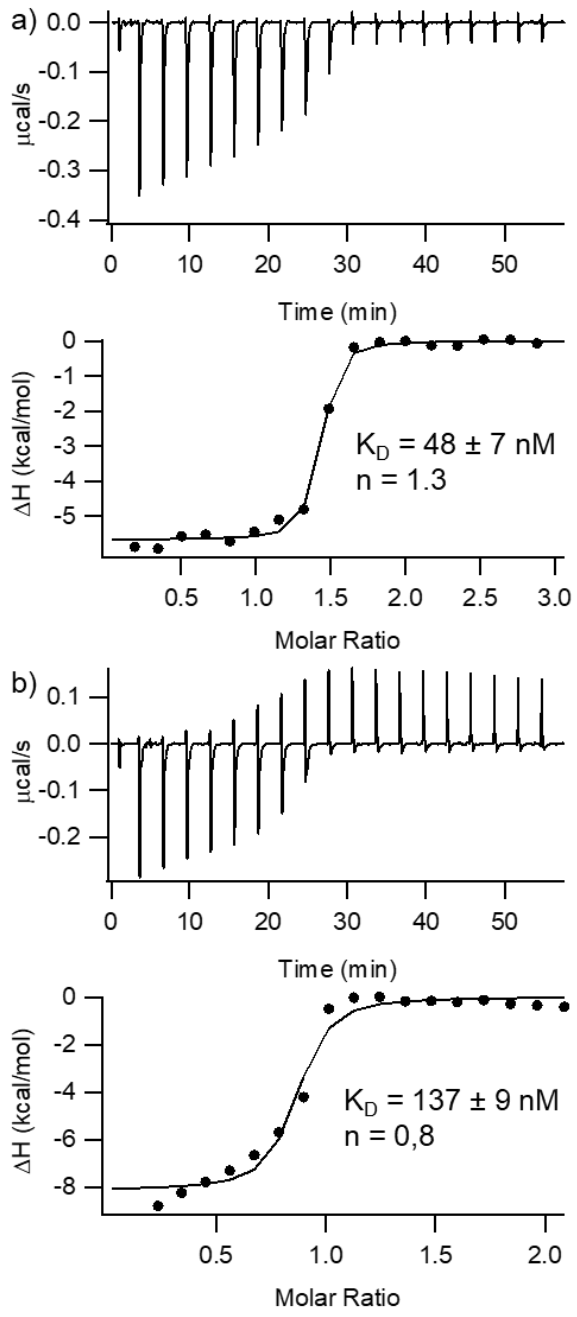

Figure 3: Isothermal calorimetric titration (ITC) of αRep (20 µM), with Citrine at 320 µM or at 230 µM for pH 7.4 (a) and pH 5.7 (b) respectively.

At physiological pH, the results are very close to previous measurements with another fluorescent protein, the EGFP (K_D = 19 ± 12 nM, n = 1.2, Figure 3a).[15] This consistency is expected as EGFP and Citrine differ by only six residues in positions 64, 65, 68, 69, 72, and 203,[3] none of those were found in interaction with the αRep, most of them being located or pointing in the barrel (Figure S1). The specific interaction was also confirmed using two negative controls. In the first one, the Citrine was replaced by mCherry, a fluorescent protein that shares the same β-barrel fold as Citrine but with a completely different residue sequence and protein surface (Figure S1). In the second one, the αRep binder used in this study has been exchanged for another binder selected against another protein target (Figure S1).[14] In both

cases, no binding was observed by ITC (Figure S2). At acidic pH, an interaction between Citrine and αRep is observed with a K_D value still in the nM range (K_D = 137 ± 9 nM, n = 0.8, Figure 3b), but 3 - 4 times higher than at physiological pH showing that the interaction is slightly less efficient.

The interaction Citrine - αRep reduces the pH sensitivity of Citrine

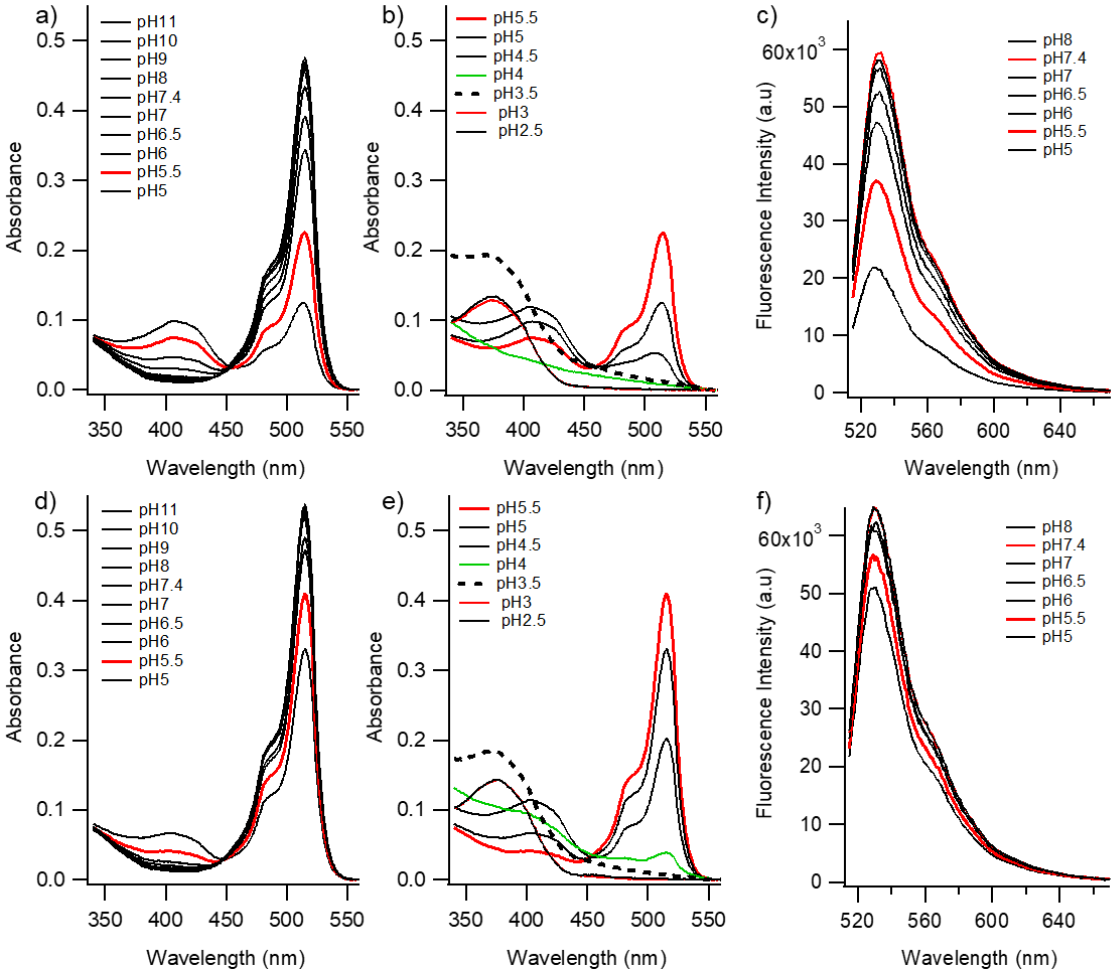

Figure 4: Absorption spectra from pH 2.5 to pH 5.5 (a and d) and from pH 5 to pH 11 (b and e)and fluorescence emission spectra upon excitation at 480 nm from pH 5 to 8 (c and e) for Citrineat 10 µM (first row) and an equimolar mixture of Citrine and αRep, 10µM each (second row). Data set of a representative experiment.

Absorption and fluorescence emission spectra of Citrine were recorded with and without αRep in a range of pH from 2.5 to 11 (Figure 4). When the pH of the solution is reduced, the decrease in the absorption band of the anionic chromophore at 515 nm is concomitant with the increase in one of the protonated chromophore at 410nm (Figure 4a and b). At pHs around pH 4.5, the baseline tends to increase in the UV, as the consequence of a strong diffusion likely due to aggregation at a pH slightly lower than the isoelectric point of the Citrine (pI = 5.5). If the pH is even lowered, a single band at 380 nm, characteristic of the denatured form of the fluorescent protein, remains (Figure 4b). In the presence of αRep, the evolution of the spectra is similar but shifted at lower pHs (Figure 4d and e). Upon excitation of the anionic chromophore at 480 nm,

the amplitude of the fluorescence emission spectra follows the same evolution as the absorption spectra without or with αRep (Figure 4c and f). We did not observe changes in the shape or the position of the spectra (Figure S3). In addition, absorbance and fluorescence intensity at the maximum of the chromophore's absorption and emission bands vary similarly with the pH showing that the change in fluorescence emission is mostly due to the decrease of the proportion of the fluorescent anionic chromophore in the solution (Figure 5a). The variations of the absorbance of the anionic chromophore with pH will be used for quantitative analysis (see below). The fluorescence lifetime of the Citrine's excited state has also been monitored at pH 7.4 and pH 5.5 (Figure S4). Without αRep, it remains constant at 3.47 ± 0.03 ns at both pHs. In the presence of two equivalents of αRep, it decreases from 3.65 ± 0.03 ns at pH 7.4 to 3.50 ± 0.03 ns at pH 5.5 (Figure S4).

From a quantitative point of view, for each condition, the pK_a, was calculated from the experimental data using a titration model (Figure 5b and c). Anions such as chloride can bind to the chromophore pocket of YFPs, influencing the equilibrium between the anionic fluorescent and protonated nonfluorescent forms of the chromophore. In most of the experiments, the chloride concentration was kept below 20 mM and the pK_a for Citrine alone (pK_a = 5.50 ± 0.03) is close to the ones of the literature without chloride.[9] The interaction of Citrine with αRep decreases its pK_a by 0.75 pH unit. In the presence of 200 mM chloride, as expected, the pK_a for Citrine alone is increased (from 5.50 to 5.70) as the one for the complex (from 4.75 to 5.25) Citrine – αRep that remains nevertheless still lower. As a control, the αRep binder is replaced by the control αRep protein that does not interact with Citrine (Figure S5). In that case, the pK_a of the mixture is the same as for the Citrine alone confirming that the observed variations of the pK_a are due to the direct interaction Citrine – αRep.

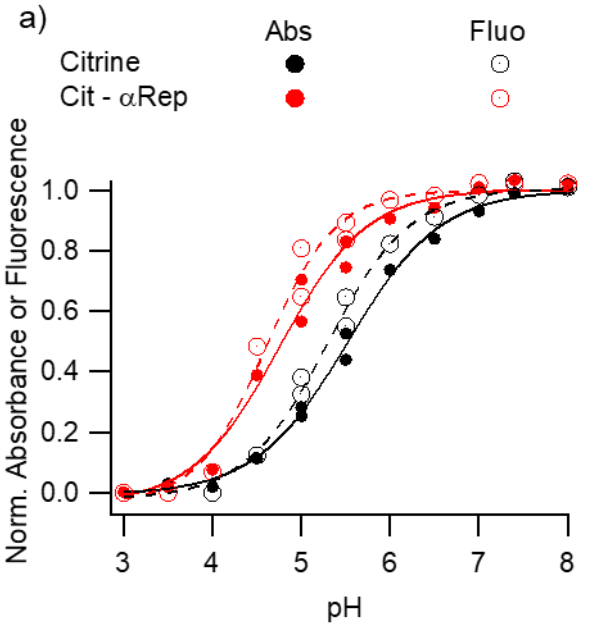
a)
Abs
Fluo
Citrine
Cit - αRep
Norm. Absorbance or Fluorescence
1.0
0.8
0.6
0.4
0.2
0.0
3
4
5
6
7
8
pH

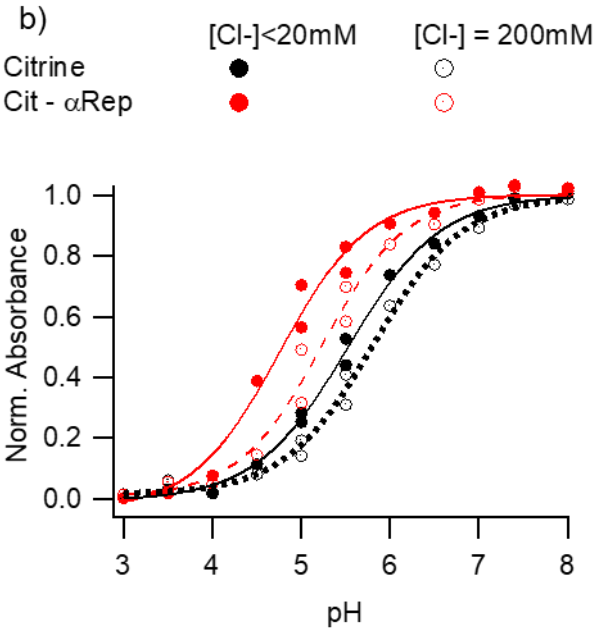
b)
[Cl-]<20mM
[Cl-] = 200mM
Citrine
Cit - αRep
Norm. Absorbance
1.0
0.8
0.6
0.4
0.2
0.0
3
4
5
6
7
8
pH

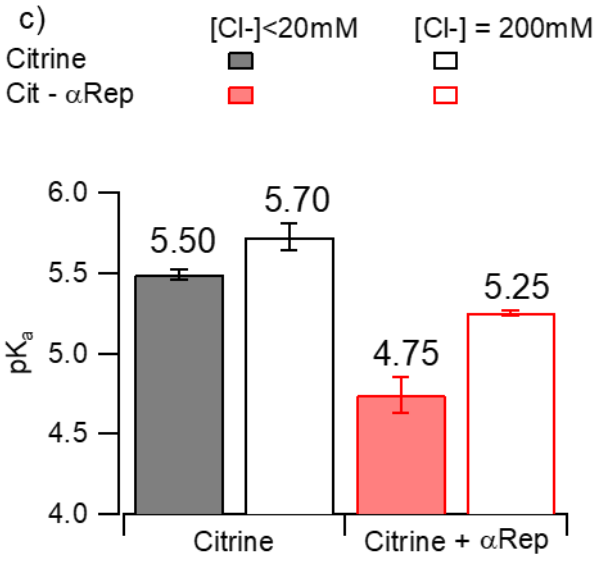
c)
[Cl-]<20mM
[Cl-] = 200mM
Citrine
Cit - αRep
6.0
5.5
5.0
4.5
4.0
pKa
5.50
5.70
4.75
5.25
Citrine
Citrine + αRep

Figure 5: (a) Comparison of the pH dependence of the absorbance at the maximum of the anionic absorption band and of the maximum fluorescence intensity at a chloride concentration below 20 mM (data set of Figure 4). (b) Comparison of the pH dependence of the absorbance at the maximum of the anionic absorption band at low and high chloride concentrations. Data with the same markers are identical in (a) and (b), all data were normalized at pH 8. (c) Average pK_a values of Citrine and a 1:1 mixture of Citrine – αRep for 3 independent experiments at $[Cl^-] < 20$ mM and 2 independent experiments at $[Cl^-] = 200$ mM.

αRep reduces the pK_a of other YFPs with close sequences

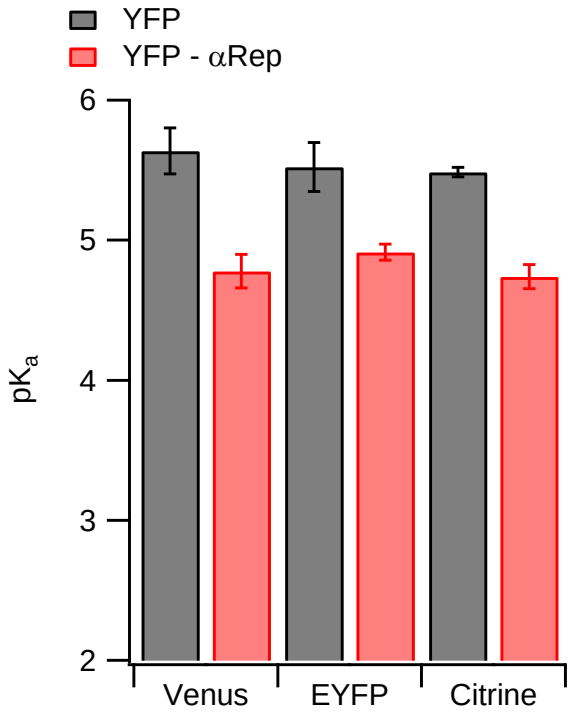

Figure 6: Average pK_a values of YFPs and an equimolar mixture YFP – αRep (n = 3, $[Cl^-] < 20$ mM. The data for Citrine are the same as in Figure 5 and added for comparison.

EYFP and Venus are popular yellow fluorescent proteins with sequences close to Citrine (Figure S1). The pK_a values of those YFPs have been measured at a low chloride concentration, alone or in interaction with αRep. As for Citrine, the interaction with αRep decreases the pK_a of the FPs showing that the effect of the interaction on pK_a can be generalized to FPs of the same family *in vitro* (Figure 6).

The interaction Citrine - αRep reduces the pK_a of Citrine in living cells

The interaction between αRep-mCherry and EGFP was proven by the colocalization of a targeted EGFP construct in a previous study.[15] Here we chose to assess the interaction between Citrine and αRep in living cells by Förster Resonance Energy Transfer (FRET) using Citrine as a fluorescent donor and mCherry fused to αRep as an acceptor. The Förster distance, at which 50% of Citrine proteins in the exited state will transfer their energy to mCherry is 59.9 Å.[3] Such a short distance is likely reached only if Citrine and αRep-mCherry form a complex. A

consequence of FRET is the decrease in the lifetime of the Citrine excited state. Here this lifetime was monitored by Fluorescence Lifetime Imaging and displayed as a color code in the images (Figure 7).

At physiological pH, when Citrine is expressed in COS7 cells, its fluorescence lifetime is 3.3 ns on average, with a low dispersion (Figure 7a and e). This value is slightly lower than recorded *in vitro* for a purified protein (see above). The intracellular pH was manipulated using nigericin, an antipore H^+/K^+ that facilitates the exchange of K^+ for H+ across membranes of living cells following a protocol optimized and validated previously.[7,21,22] As a consequence, there is a dissipation of the proton gradient (ΔpH) across the cell membranes and the pH inside cells equilibrate with the one outside. When the intracellular pH is decreased using a KCl-rich buffer at pH 6 in the presence of nigericin,[7] the lifetime is kept at a close value, consistent with *in vitro* data above (Figure 7b and e). When Citrine and a fusion αRep-mCherry are co-expressed in the COS7 cells with two independent plasmids, the lifetimes were shorter and their distribution was spread over 1.5 ns (Figure 7c, d and e). There is a clear FRET between Citrine and mCherry fused to αRep: Citrine and αRep interact in live cells at physiological and acidic pH. The spreading of the lifetime is cell-dependent and strongly related to the relative amount of αRep-mCherry. The fluorescence intensity in the acceptor channel, proportional to αRep-mCherry expression levels in the cell, has been monitored. The evolution of the FRET efficiency with the fluorescence intensity of αRep-mCherry follows a saturation curve (Figure 7f). For lower fluorescence values, the amount of αRep-mCherry in the cell is too low to interact with all the Citrine proteins. Some Citrine are still free leading to a low apparent FRET efficiency. For higher fluorescence values, all Citrine are in interaction with αRep-mCherry, and the apparent FRET efficiency is reaching a maximum. Altogether, these results show an efficient interaction of Citrine with αRep-mCherry in the living cell consistently with the first observations of interactions between EGFP and αRep.[15] In addition, they also show that the FRET efficiency is the same at neutral and acidic pHs. In consequence, the decrease of fluorescence intensity due to FRET from Citrine to mCherry is expected to be the same at all pHs tested in the next experiments in living cells.

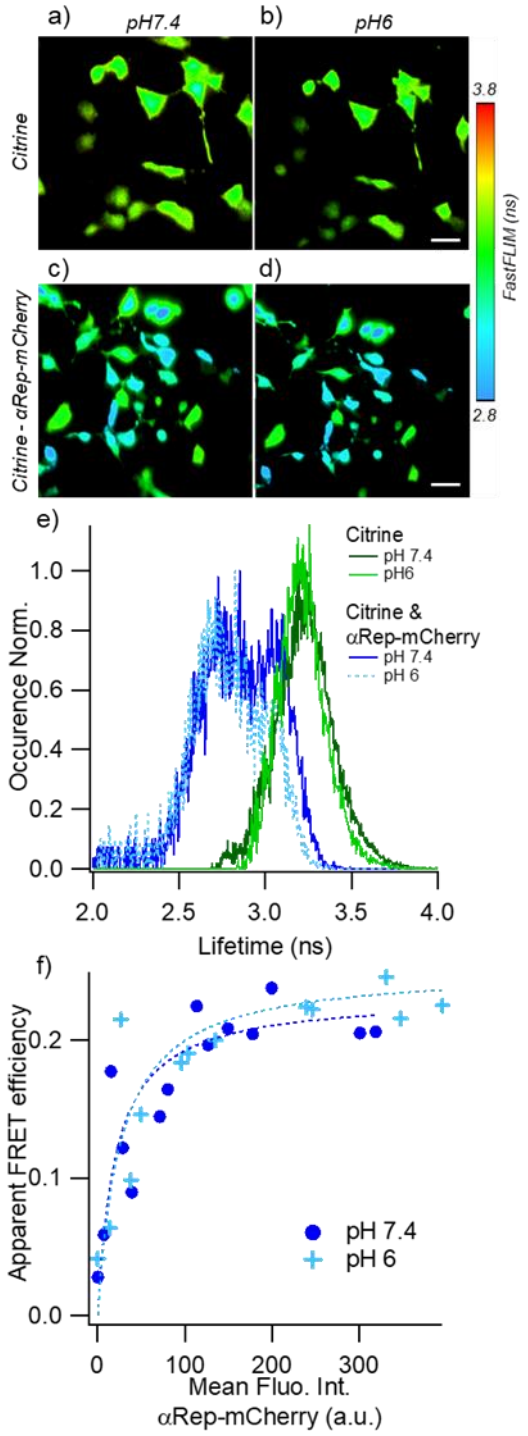

Figure 7: Fluorescence lifetime images (FastFLIM) of COS7 cells expressing either Citrine (first row) or Citrine and αRep-mCherry (second row) at pH 7.4 in PBS (a, c) or at pH 6 (b, d), scale bar 15 µm. (e) Lifetime distribution in all pixels in the four FastFLIM images. (f) Variation of the apparent FRET efficiency calculated for 16 cells in images c and d with the fluorescence intensity of αRep-mCherry in the same cells (one point represents one cell).

In a second step, to monitor the effect of the binding of αRep-mCherry on the pH sensitivity of Citrine's fluorescence properties, it is necessary to monitor the fluorescence intensity of Citrine in living cells at various pHs. An example of intensity variations between neutral and acidic pHs is shown in Figure 8a-d, and αRep clearly limits those variations (Figure S6 for quantitative analysis of intensity images:). Nevertheless, flow cytometry is the method of choice to explore a large cell population and have a statistical and accurate approach to the average fluorescence intensities. In addition, among the cell population co-expressing Citrine and αRep-mCherry, flow cytometry offers the possibility to choose cells expressing both proteins, based on their fluorescence intensity in the yellow (Citrine) and in the red channels (mCherry) (Figure S7). The amounts of plasmids for transfection have been chosen to have, on average, Citrine and αRep-mCherry expression levels at which the FRET efficiency is maximum in FLIM, most of Citrine being in a bound form. The average fluorescence intensity of Citrine was calculated for various intracellular pHs (Figure 8e). First, it depends on the FRET efficiency that is pH-independent (Figure 7f). So, we could estimate that the FRET will impact the Citrine brightness in the same proportion at all pHs. Second, it is also proportional to the fraction of the proteins with an anionic and fluorescent chromophore, which is pKa dependent. At pH 6.5, the fluorescence starts to decrease with a drop of 35% at pH 5.5 for Citrine alone. In the presence of αRep-mCherry, at pH 5.5, the relative drop of fluorescence to pH 7.4 is limited to 15%. This shows that the interaction Citrine – αRep limits the protonation of the Citrine's chromophore in living cells, as *in vitro*.

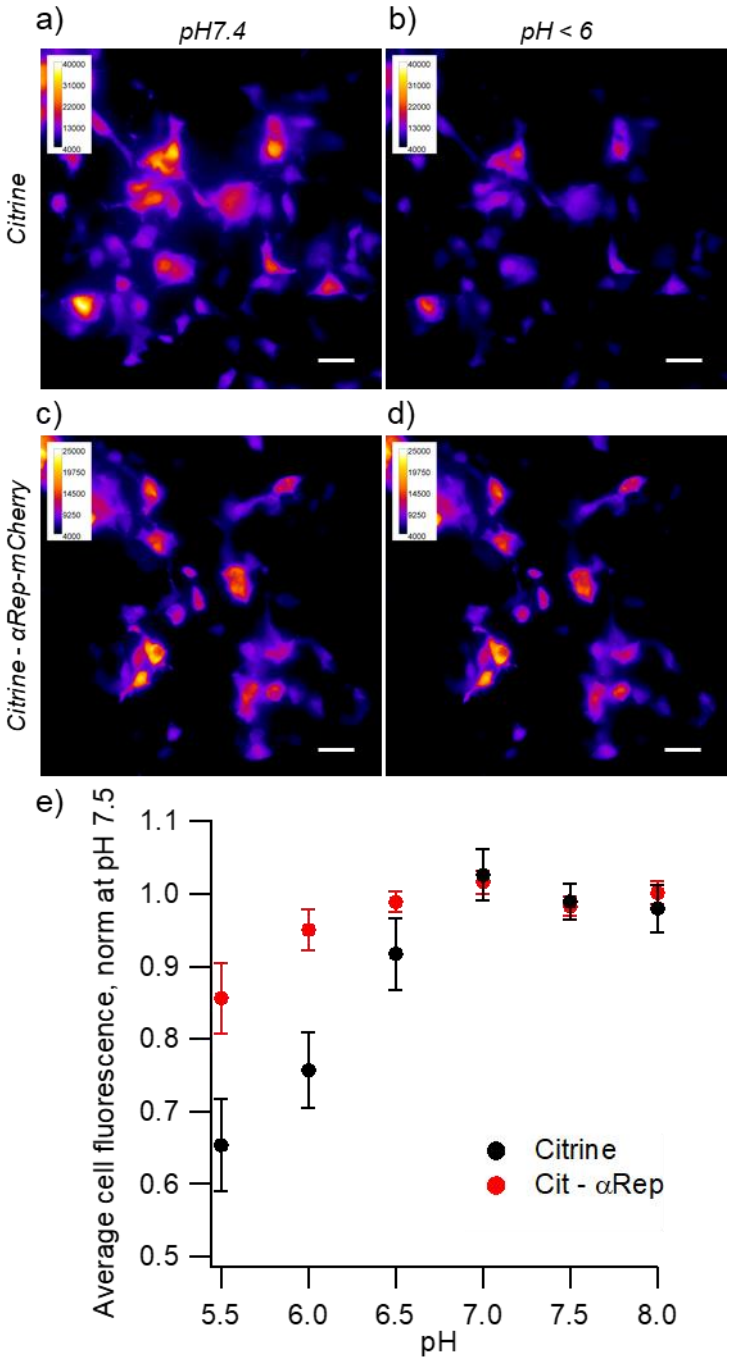

Figure 8: Wide-field fluorescence microscopy images of COS7 cell expressing Citrine (first row) or Citrine and αRep – mCherry (second row) at pH 7.4 (a, c) and pH < 6 (b, d), scale bar 20 µm. Histograms of fluorescence intensities in each image and the αRep – mCherry intensity image are in Figure S6. (e) Average cellular fluorescence of Citrine for COS7 cells expression of either Citrine or both Citrine and αRep – mCherry. In the latter case, only cells expressing both Citrine and αRep – mCherry were chosen based on their fluorescence intensities. Data from each experiment were normalized at pH 7.5 and averaged (n = 4).

Discussion

Our results show that αRep binds Citrine at physiological pH with a very high affinity and this binding stabilizes the Citrine's as shown by an increased T_m. Furthermore, as the shape and position of the absorption and emission spectra do not change, this suggests that the binding of αRep does not induce significant modifications in the electrostatic field in the cavity around the chromophore.[23] In order to understand the modification induced by the binding of αRep on Citrine's structure, the available X-ray structures of EGFP and EGFP- αRep complex can be compared. The RMSD profile of each Cα atom of EGFP in the EGFP- αRep complex *vs*. EGFP shows that there is no substantial global influence on the overall fold of EGFP as it has already been observed for interaction with nanobodies (Figure S8).[12] The binding rather influences the strength of intra-molecular bonds in the *β*-barrel as shown by the T_m variation. Nevertheless, the small fluctuations on the RMSD profile are observed in the flexible turns mainly between the 7th and 8th as well as the 8th and 9th strands, with positions Q157 and G174 being mainly affected. This is consistent with the direct interaction of Q157 with N160 and E163 in the αRep.[15] Also, G174 is nearby S175 and V176 both interacting with αRep's Y60 and L63.[15] In addition, the fluorescence lifetime of the chromophore in the bound form is higher than for the free Citrine (3.65 ± 0.03 ns and 3.47 ± 0.03 ns respectively). This is a direct consequence of the rigidification of the chromophore in its pocket upon binding either through an increase of the compaction around the chromophore or a strengthening of the H-bond network.[19,24] The X-ray structures for the complex and EGFP have different resolutions, 3.40 Å and 1.65 Å, respectively. Moreover, the resolution of the complex structure is too low to see the water molecules and thus follow the extended H-bond network around the chromophore. So, the changes observed by comparing the two structures are too small to provide any conclusions that would pinpoint the residues in the rigidification (Figure S9). As a consequence, we postulate, that the presence of αRep mainly induces a cooperative effect that limits the global dynamics of the protein and of its chromophore. At pH 5.5, the T_m of Citrine is decreased and the one of αRep is increased: the intramolecular forces in both proteins are modified. The structural changes in both partners have a direct impact on the stability of the complex that unfolds at a lower T_m at acidic pH, the binding being also slightly less efficient but still in the nM range. Nevertheless, the bound form has a higher T_m than Citrine alone, showing again a global structuring effect of αRep on Citrine. We know from the absorption measurements, that at pH 5.5, some Citrine have a protonated and nonfluorescent chromophore. The ones remaining anionic and fluorescent have the same fluorescence lifetime as the fluorescent form of the Citrine alone at pH 5.5. At this low pH, our results point out that the binding has no major impact on the dynamic of the chromophore in its pocket. So, the structuring effect is not as strong as at physiological pH. To conclude, all these effects are likely behind the lowering of their pK_a, making Citrine still fluorescent and thus usable at significantly more acidic pHs. The good expression and solubility of αRep in living cells enabled us to confirm this effect in COS7 cells. We also observed that the chloride sensitivity of Citrine is not reduced in the Citrine - αRep complex. Thus, the latter does not significantly interfere with the diffusion pathway of chloride ions toward the well-known halogen cavity near the chromophore of YFPs.[25,26] Indeed, chloride ions are likely to use the channel formed by the network of water molecules observed in KillerRed[27] or avGFP and TurboGFP[28] and connecting the lids of the

β-barrel to the chromophore vicinity. As expected from the crystal structure of the complex, the lid remains accessible to chloride in the presence of αRep. (Figure 1).

Conclusion

The binding of αRep to Citrine is efficient, even in acidic solutions and at acidic pHs in living cells. It increases the stiffness around the chromophore at physiological pH and influences its protonation, likely by stabilizing the H-bond networks around the anionic chromophore. As a consequence, the pK_a of the Citrine is decreased, maintaining high fluorescence even at acid pH down to 5.5 in living cells, allowing a brighter label at lower pH values. More generally, this study demonstrates the feasibility of modulating the properties of YFPs through the binding of an αRep. The next step will be the design of FRET-based biosensors to monitor biochemical events in acidic environments like the phagosomes of phagocytic cells, such as neutrophils' cellular modal.[29,30] Using as an acceptor a Citrine-αRep fusion in pair with Aquamarine or mTurquoise2 will pave the way for the next generation of such biosensors adapted for acid environments. Finally, our work opens up the possibility of using both pK_a and lifetime measurements to screen for other αReps with completely different binding modes, potentially leading to greater effects not only on pK_a and pH sensitivity but also on other parameters such as brightness or photostability.

References

[1] P. Dedecker, F. C. De Schryver, J. Hofkens, *J. Am. Chem. Soc.* **2013**, *135*, 2387–2402.
[2] M. D. Vecchia, A. Conte-Daban, B. Cappe, W. Vandenberg, P. Vandenabeele, F. B. Riquet, P. Dedecker, *ACS Sens.* **2022**, *7*, 2920–2927.
[3] T. J. Lambert, *Nat Methods* **2019**, *16*, 277–278.
[4] O. Griesbeck, G. S. Baird, R. E. Campbell, D. A. Zacharias, R. Y. Tsien, *J Biol Chem* **2001**, *276*, 29188–29194.
[5] J. R. Casey, S. Grinstein, J. Orlowski, *Nat Rev Mol Cell Biol* **2010**, *11*, 50–61.
[6] H.-H. Tsai, W. Schmidt, *Nat. Plants* **2021**, *7*, 106–115.
[7] D.-B. Betolngar, M. Erard, H. Pasquier, Y. Bousmah, A. Diop-Sy, E. Guiot, P. Vincent, F. Mérola, *Anal Bioanal Chem* **2015**, *407*, 4183–4193.
[8] D. M. Chudakov, M. V. Matz, S. Lukyanov, K. A. Lukyanov, *Physiol Rev***2010**, *90*, 1103–1163.
[9] Y. Bousmah, H. Valenta, G. Bertolin, U. Singh, V. Nicolas, H. Pasquier, M. Tramier, F. Merola, M. Erard, *ACS Sens.* **2021**, *6*, 3940–3947.
[10] M. Eshaghi, G. Sun, A. Grüter, C. L. Lim, Y. C. Chee, G. Jung, R. Jauch, T. Wohland, S. L. Chen, *Angew Chem Int Ed* **2015**, *54*, 13952–13956.
[11] T. Roebroek, S. Duwé, W. Vandenberg, P. Dedecker, *IJMS* **2017**, *18*, 2015.
[12] A. Kirchhofer, J. Helma, K. Schmidthals, C. Frauer, S. Cui, A. Karcher, M. Pellis, S. Muyldermans, C. S. Casas-Delucchi, M. C. Cardoso, H. Leonhardt, K.-P. Hopfner, U. Rothbauer, *Nat Struct Mol Biol* **2010**, *17*, 133–138.
[13] A. Urvoas, A. Guellouz, M. Valerio-Lepiniec, M. Graille, D. Durand, D. C. Desravines, H. Van Tilbeurgh, M. Desmadril, P. Minard, *J Mol Biol* **2010**, *404*, 307–327.
[14] A. Guellouz, M. Valerio-Lepiniec, A. Urvoas, A. Chevrel, M. Graille, Z. Fourati-Kammoun, M. Desmadril, H. Van Tilbeurgh, P. Minard, *PLoS ONE* **2013**, *8*, e71512.
[15] A. Chevrel, A. Urvoas, I. L. De La Sierra-Gallay, M. Aumont-Nicaise, S. Moutel, M. Desmadril, F. Perez, A. Gautreau, H. Van Tilbeurgh, P. Minard, M. Valerio-Lepiniec, *Bioscience Reports* **2015**, *35*, e00223.
[16] Y. Nasu, Y. Shen, L. Kramer, R. E. Campbell, *Nat Chem Biol* **2021**, *17*, 509–518.
[17] L. Alvarez, C. H. Levin, F. Merola, T. Bizouarn, H. Pasquier, L. Baciou, F. Rusconi, M. Erard, *Photochem Photobiol* **2010**, *86*, 55–61.
[18] P. J. Cranfill, B. R. Sell, M. A. Baird, J. R. Allen, Z. Lavagnino, H. M. de Gruiter, G.-J. Kremers, M. W. Davidson, A. Ustione, D. W. Piston, *Nat Meth* **2016**, *13*, 557–562.
[19] M. Erard, A. Fredj, H. Pasquier, D.-B. Beltolngar, Y. Bousmah, V. Derrien, P. Vincent, F. Merola, *Mol. BioSyst.* **2013**, *9*, 258–267.
[20] C. S. Ziegler, L. Bouchab, M. Tramier, D. Durand, F. Fieschi, S. Dupré-Crochet, F. Mérola, O. Nüße, M. Erard, *J. Biol. Chem.* **2019**, *294*, 3824–3836.
[21] S. Poëa-Guyon, H. Pasquier, F. Mérola, N. Morel, M. Erard, *Anal Bioanal Chem* **2013**, *405*, 3983–3987.
[22] H. Valenta, S. Dupré-Crochet, M. Abdesselem, T. Bizouarn, L. Baciou, O. Nüsse, A. Deniset-Besseau, M. Erard, *BBA - Mol Cell Res* **2022**, *1869*, 119276.
[23] M. Drobizhev, P. R. Callis, R. Nifosì, G. Wicks, C. Stoltzfus, L. Barnett, T. E. Hughes, P. Sullivan, A. Rebane, *Sci Rep* **2015**, *5*, 13223.
[24] K. Nienhaus, G. U. Nienhaus, *Methods Appl. Fluoresc.* **2022**, *10*, 042002.
[25] R. M. Wachter, D. Yarbrough, K. Kallio, S. J. Remington, *J Mol Biol* **2000**, *301*, 157–171.
[26] S. Jayaraman, P. Haggie, R. M. Wachter, S. J. Remington, A. S. Verkman, *J Biol Chem* **2000**, *275*, 6047–6050.
[27] P. Carpentier, S. Violot, L. Blanchoin, D. Bourgeois, *FEBS Letters* **2009**, *583*, 2839–2842.

[28] B. Li, R. Shahid, P. Peshkepija, M. Zimmer, *Chemical Physics* **2012**, *392*, 143–148.
[29] L. Nault, L. Bouchab, S. Dupré-Crochet, O. Nüße, M. Erard, *Antioxidants & Redox Signaling* **2016**, *25*, 564–576.
[30] H. Valenta, M. Erard, S. Dupré-Crochet, O. Nüβe, in *Molecular and Cellular Biology of Phagocytosis* (Ed.: M.B. Hallett), Springer International Publishing, Cham, **2020**, pp. 153–177.

Acknowledgments

The authors thank CNRS and Université Paris Saclay for their financial support. This work was also supported by LabEx PALM, Grant ANR-10-LABX-0039-PALM. The present work has benefited from the SpICy microscopy facility of ICP for flow cytometry and FLIM and the facility of macromolecular interactions (PIM platform) of I2BC, supported by French Infrastructure for Integrated Structural Biology (FRISBI) ANR-10-INBS-05.

Supplementary figures.

a)

```
mCherry   1 MVSKGEEDNMAIIKEFMRFKVHMEGSVNGHEFEIEGEGEGRPYEGTQTAKLKVTKGGP
EGFP      1 MVSKGEE----LFTGVVPILVELDGDVNGHKFSVSGEGEGDATYGKLTLKF-ICTTGK
Venus     1 MVSKGEE----LFTGVVPILVELDGDVNGHKFSVSGEGEGDATYGKLTLKL-ICTTGK
Citrine   1 MVSKGEE----LFTGVVPILVELDGDVNGHKFSVSGEGEGDATYGKLTLKF-ICTTGK
EYFP      1 MVSKGEE----LFTGVVPILVELDGDVNGHKFSVSGEGEGDATYGKLTLKF-ICTTGK

mCherry  59 LPFAWDILSPQFMYGSKAYVKHPADIP--DYLKLSFPEGFKWERVMNFEDGGVVTVTQ
EGFP     54 LPVPWPTLVTTLTYGVQCFSRYPDHMKQHDFFKSAMPEGYVQERTIFFKDDGNYKTRA
Venus    54 LPVPWPTLVTTLGYGLQCFARYPDHMKQHDFFKSAMPEGYVQERTIFFKDDGNYKTRA
Citrine  54 LPVPWPTLVTTFGYGLMCFARYPDHMKQHDFFKSAMPEGYVQERTIFFKDDGNYKTRA
EYFP     54 LPVPWPTLVTTFSYGLQCFARYPDHMKQHDFFKSAMPEGYVQERTIFFKDDGNYKTRA

mCherry 115 DSSLQDGEFIYKVKLRGTNFPSDGPVMQKKTMGWEASSERMY----PEDGALKGEIKQ
EGFP     112 EVKFEGDTLVNRIELKGIDFKEDGNILGHK-LEYNYNSHNVYIMADKQKNGIKVNFKI
Venus    112 EVKFEGDTLVNRIELKGIDFKEDGNILGHK-LEYNYNSHNVYITADKQKNGIKANFKI
Citrine  112 EVKFEGDTLVNRIELKGIDFKEDGNILGHK-LEYNYNSHNVYIMADKQKNGIKVNFKI
EYFP     112 EVKFEGDTLVNRIELKGIDFKEDGNILGHK-LEYNYNSHNVYIMADKQKNGIKVNFKI

mCherry 169 RLKLKDGG-----HYDAEVKTTYKAKKPVQLPGAYNVNIKLDIT---SHNEDYTIVEQ
EGFP     169 RHNIEDGSVQLADHYQQNTPI---GDGPVLLPDNHYLSTQSALSKDPNEKRDHMVLLE
Venus    169 RHNIEDGGVQLADHYQQNTPI---GDGPVLLPDNHYLSYQSALSKDPNEKRDHMVLLE
Citrine  169 RHNIEDGSVQLADHYQQNTPI---GDGPVLLPDNHYLSYQSALSKDPNEKRDHMVLLE
EYFP     169 RHNIEDGSVQLADHYQQNTPI---GDGPVLLPDNHYLSYQSALSKDPNEKRDHMVLLE

mCherry 219 YERAEGRHSTGGMDELYK
EGFP     224 FVTAAG--ITLGMDELYK
Venus    224 FVTAAG--ITLGMDELYK
Citrine  224 FVTAAG--ITLGMDELYK
EYFP     224 FVTAAG--ITLGMDELYK
```

b)

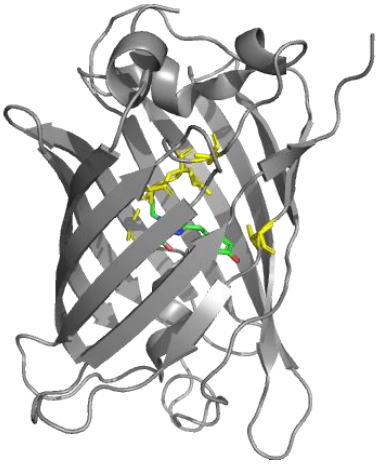

c)

```
bGFPC       1 MRGSHHHHHHTDPEKVEMYIKNLQDDSMRVRYNAATALGKIGDERAVEPLIKALKD
bNCS324-16  1 MRGSHHHHHHTDPEKVEMYIKNLQDDSYFVRRAAAAALGKIGDERAVEPLIKALKD

bGFPC      57 EDGYVRLEAAEALGEIGDERAVEPLIKALKDEDPDVRSEAALALGKIGDERAVEPL
bNCS324-16 57 EDRFVR----------------------------------SSAAYALGEIGDERAVEPL

bGFPC     113 IKALKDEDRYVRMAAAWALGKIGGERVRAAMEKLAETGTGFARKVAVNYLETHKSL
bNCS324-16 82 IKALKDEDWFVRRAAAVALGEIGGERVRAAMEKLAETGTGFARKVAVNYLETHKSL

bGFPC     169 IS
bNCS324-16 138 IS
```

Figure S1 Amino acid sequences of fluorescent proteins and binders: (a) Sequence alignment of mCherry, EGFP, Venus, Citrine, and EYFP, the chromophore sequence is in the green box. (b) EGFP structure (pdb 4XVP) is in grey and residues mutated in Citrine are in yellow, all facing the inside of the barrel. The residue 65 in the chromophores is also different. (c) Sequence alignment of binders, bGFPC called **αRep** and bNCS324-16 called **control αRep**

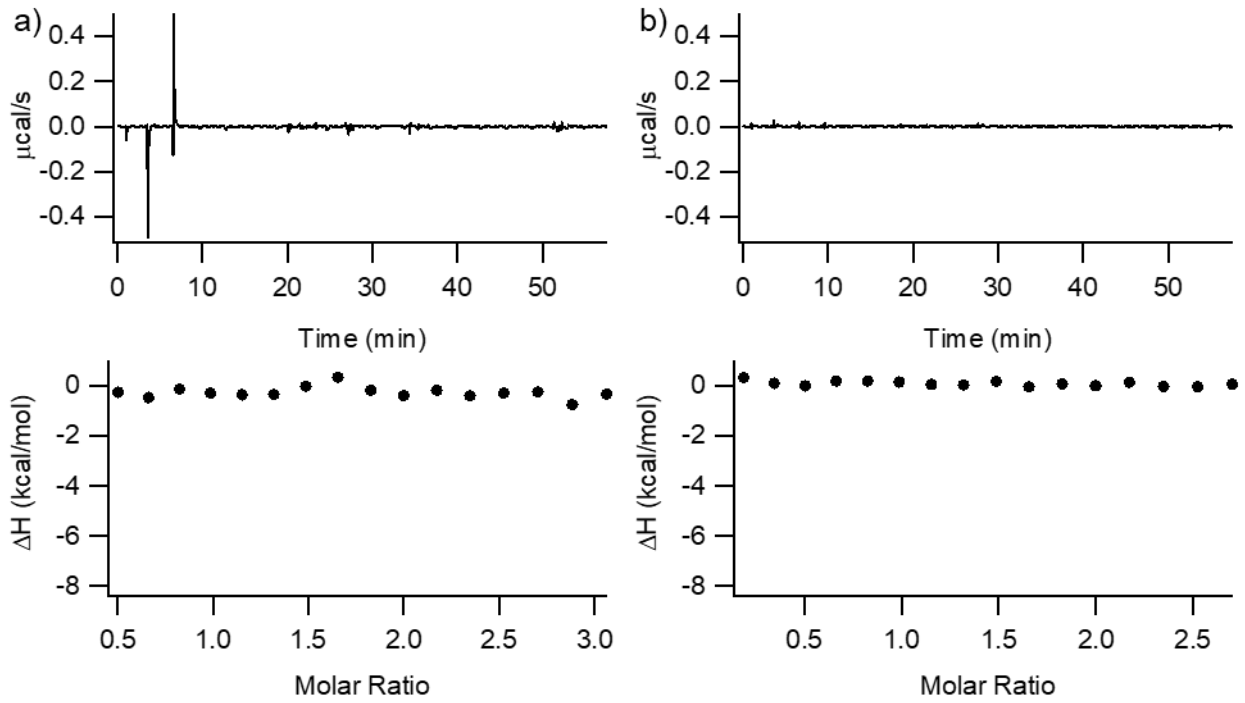

Figure S2: Raw signals of ITC obtained at pH 7.4 of Citrine (320 µM) in control αRep (16.5 µM) (a) and mCherry (320 µM) in αRep (14.3 µM) (b).

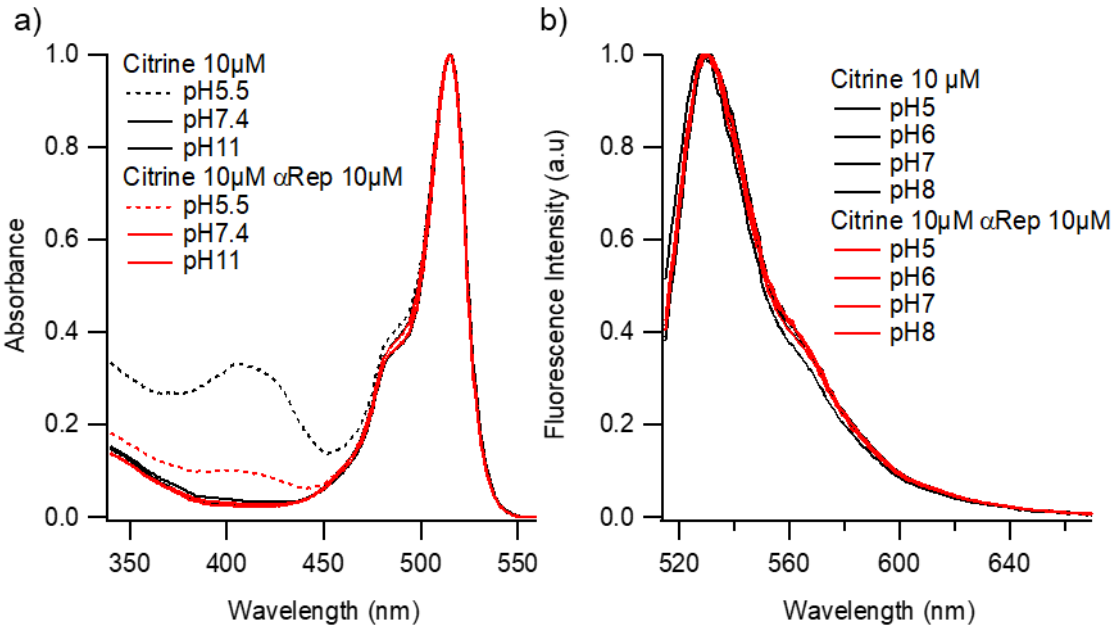

Figure S3: Overlay of normalized absorption (a) and fluorescence emission(b) spectra of Citrine (10µM) and a mixture 1:1 Citrine - αRep, 10 µM each.

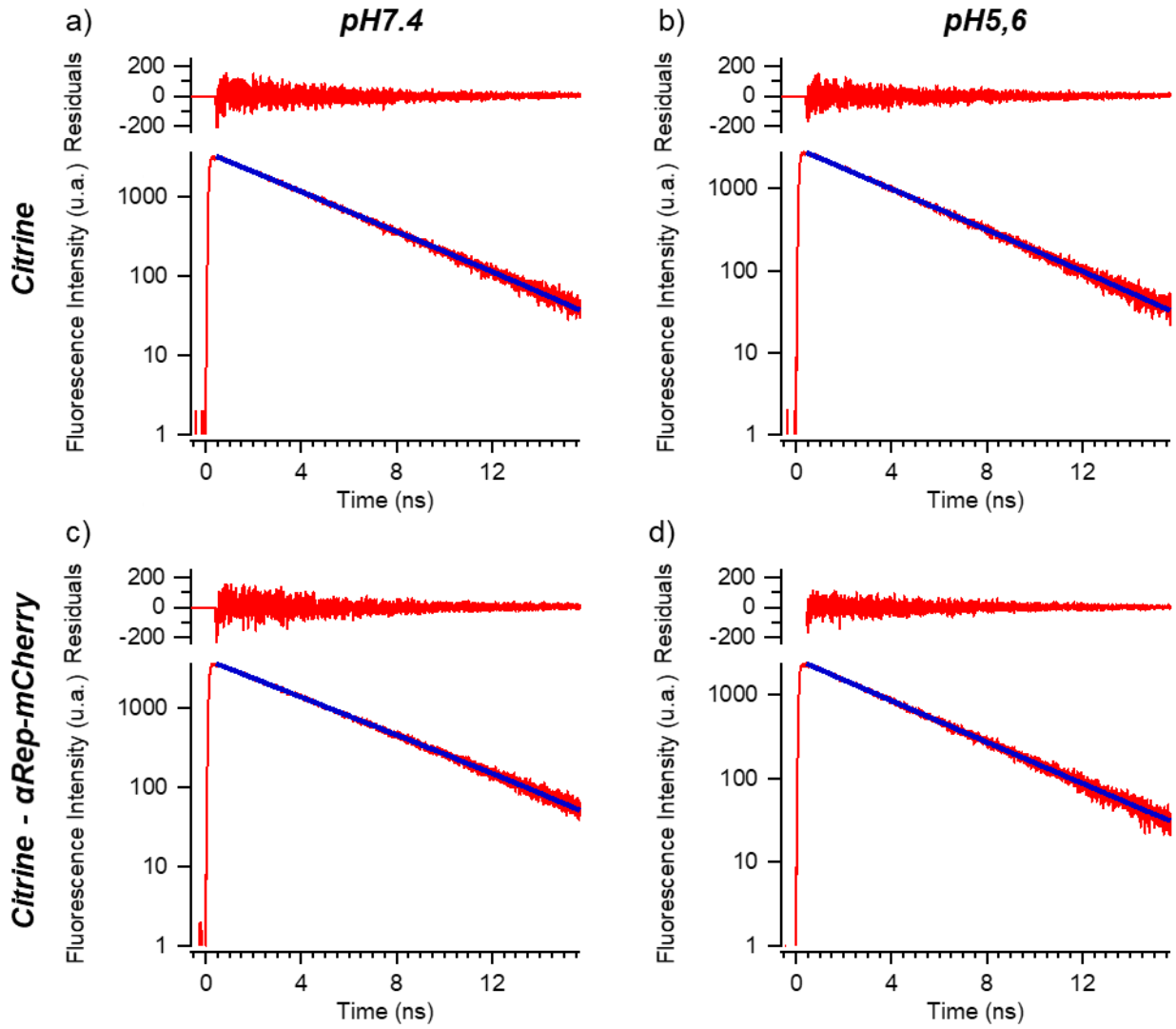

Figure S4: Fluorescence decays (red), monoexponential fit (blue), and residuals for Citrine (a, b) and a mixture 1:1 Citrine – αRep (c,d) at pH 7.4 (a,c) and pH5.6 (b,d).

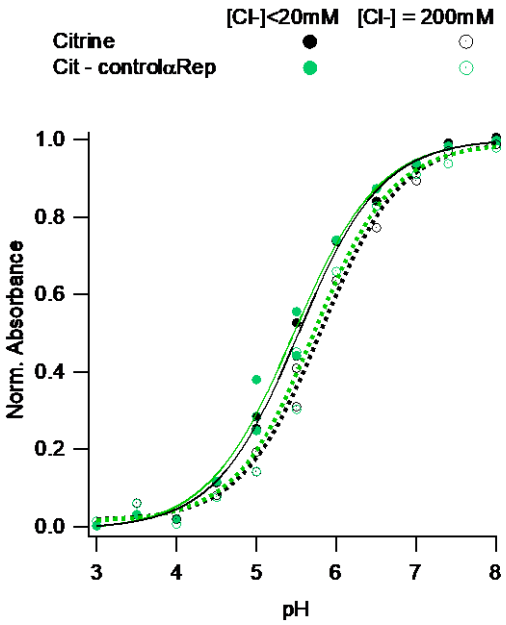

Figure S5: Chloride effect on the pH dependence of the absorbance at the maximum of the anionic band of the chromophore. Experimental data were normalized to 100% at the maximum of their analytical fits.

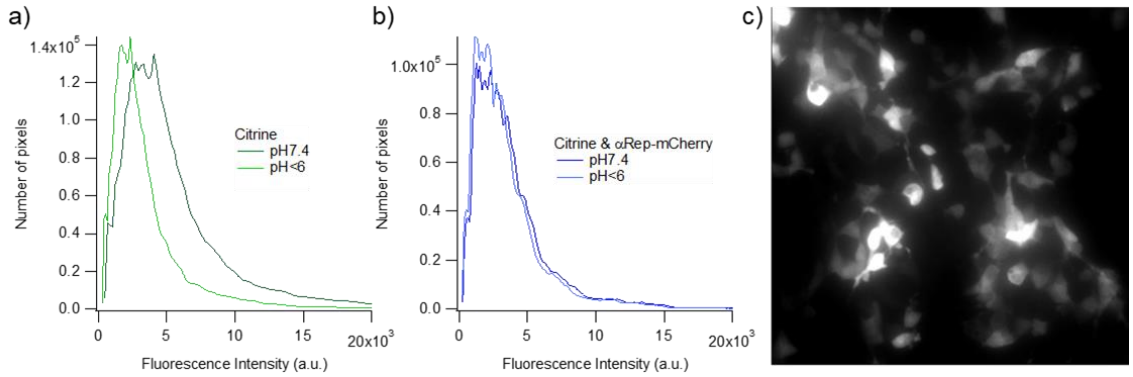

Figure S6: Histograms of fluorescence intensities in each image at pH 7.4 and pH < 6 for Citrine alone (a) and a co-expression of Citrine and αRep – mCherry (b). Intensity image of mCherry at pH 7.4 for the same field of view as Figure 8c.

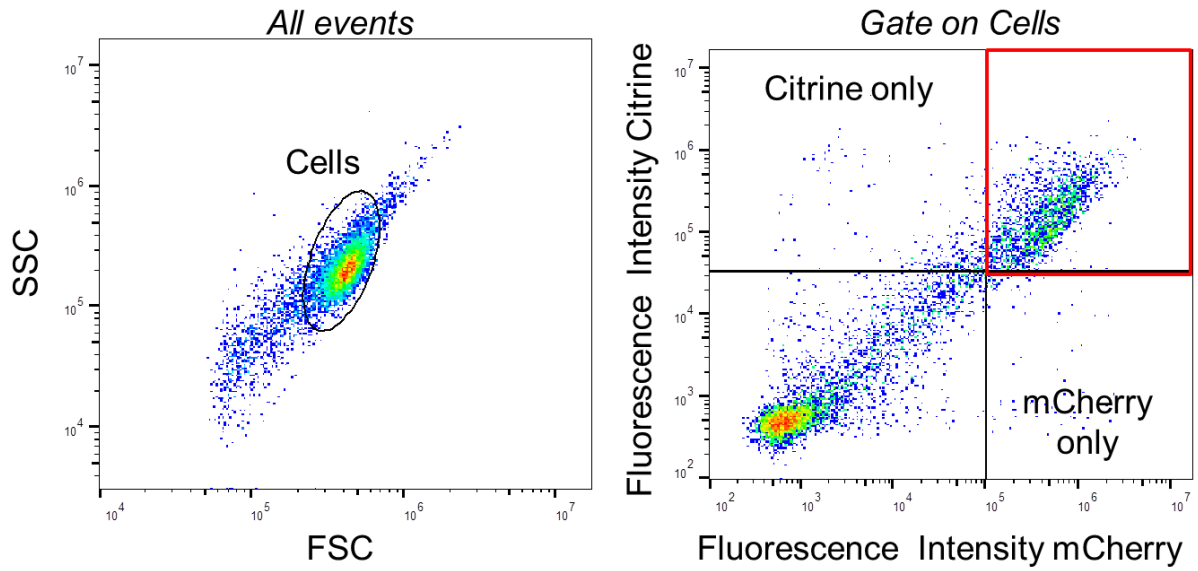

Figure S7: Gating strategy to cytometry experiments for a co-expression of Citrine and αRep – mCherry (data at pH 7.4). The average Citrine fluorescence is calculated for the events in the red square.

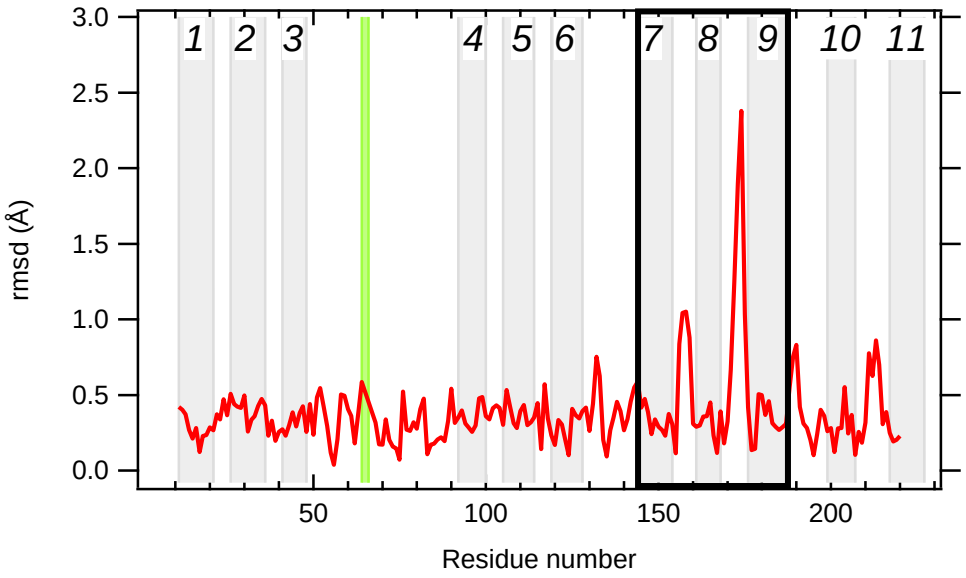

Figure S8: RMSD profile for each Cα atoms of EGFP in the EGFP - αRep complex (pdb 4XVP) vs. EGFP (pdb 6YLQ). The position of the eleven β-strands and of the chromophore are indicated in grey and green, respectively. The black box represents the binding area of αRep.

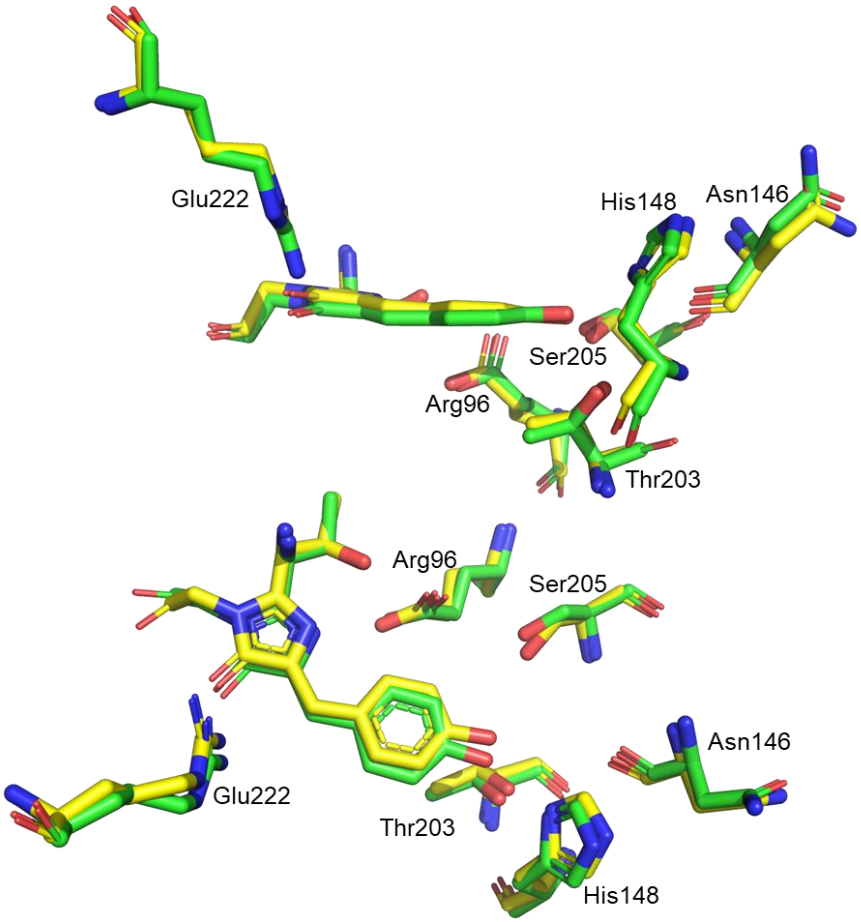

Figure S9: Structures of the chromophore in its pocket for EGFP (green, pdb 6YLQ) and EGFP - αRep complex (yellow, pdb 4XVP).